IEEE Access
Multidisciplinary : Rapid Review : Open Access Journal

Received 16 April 2024, accepted 7 May 2024, date of publication 13 May 2024, date of current version 31 May 2024.

Digital Object Identifier 10.1109/ACCESS.2024.3400322

RESEARCH ARTICLE

ASMC and ARSMC Cascaded Controller Design for QUAVs With Time-Varying Load and Unknown Disturbances

FALU WENG[1], HUI WEI[1], JIANYI HU[2], LU ZENG[1], AND RUCHUN WEN[1]

[1]School of Electrical Engineering and Automation, Jiangxi University of Science and Technology, Ganzhou, Jiangxi 341000, China

[2]Jiangxi New Energy Technology Institute, Xinyu, Jiangxi 338000, China

Corresponding authors: Hui Wei (897044594@qq.com) and Lu Zeng (zenglu@jxust.edu.cn)

This work was supported in part by the National Natural Science Foundation under Grant 62363013 and Grant 72164016, and in part by Jiangxi Provincial Natural Science Foundation of China under Grant 20202BABL202011.

ABSTRACT In this paper, cascaded controllers, which combine adaptive sliding mode control and recursive techniques, are presented to control quadrotor unmanned aerial vehicles with time-varying load and unknown disturbances. In the outer-loop control subsystem, an adaptive sliding mode controller, which includes adaptive laws estimating the time-varying load and unknown disturbances, is presented to control the position of the quadrotor. In the inner-loop control subsystem, an adaptive recursive sliding mode controller, which includes a self-turning law estimating the unknown inner-loop disturbances, is designed to control the attitude of the quadrotor. Moreover, a nonsingular terminal sliding mode surface is used to converge the tracking error of attitude angles to zero in finite time; and an integral sliding mode surface is designed in the adaptive recursive sliding mode controller to improve the attitude control performance of the quadrotor. Simultaneously, adaptive gain adjustment laws were applied to estimate those unknown upper bounds of the disturbances in the system. In the end, the efficiency and feasibility of the proposed control method are demonstrated by some computer simulations.

INDEX TERMS Unmanned aerial vehicle, time-varying load, trajectory tracking control, adaptive control, unknown disturbance.

I. INTRODUCTION

Over the past several years, quadrotor unmanned aerial vehicles (QUAVs) have attracted extensive attentions and have been widely used in the precision agriculture, aerial photography and some civil entertainment fields owing to their advantages, such as vertical takeoff, landing and hovering flight, etc. [1], [2], [3], [4]. It is well known that QUAVs are under-actuated, strongly nonlinear and coupling systems, so the stability analysis and controller design for QUAVs are still challenging [5], [6]. Fortunately, as to these issues, some efforts have been tried by scholars, and lots of results were achieved [7], [8], [9]. Moreover, there are numerous control strategies, such as, Proportional Integral Differential (PID) [10], Active Disturbance Rejection Control (ADRC) [11], Sliding Mode Control (SMC) [12], etc., have been proposed for the control of QUAVs.

It is worth noting that PID controllers are widely used in the control of all kinds of devices in industries, agricultures and other fields, due to its advanced advantages, such as simplicity principle, easy to implement, independent control parameters, etc. [13], [14], [15]. However, some performances of the PID-controlled systems were seriously declined in the presence of some parameter uncertainties or disturbances in the systems [16]. In order to mitigate the impact of disturbances on the flying performance of QUAVs, an ADRC was proposed in [17]. The ADRC, which has an Extended State Observer(ESO), can online estimate and compensate the internal and external disturbances [18]. The effectiveness of the ESO can be found in the following references ([19], [20], [21], [22], [23], [24]. For example, a fixed-time ESO was proposed in [19] to observe the

The associate editor coordinating the review of this manuscript and approving it for publication was Mou Chen.

unmeasurable velocity and unknown external disturbances. Liu et al. suggested a nonlinear adaptive backstepping controller with ESO for trajectory tracking of a QUAV subject to multiple disturbances in [20]. In [22], a nonsingular terminal sliding mode controller combined with an ESO was employed for the attitude control of a QUAV. Du et al. integrated a two-stage Kalman filter (TSKF) with an ESO to further compensate for the influences of factor estimation errors [23].

In practical systems, the variations of the disturbances are often random and complex, thus, it is almost impossible for researchers to obtain an ESO to accurately estimate those disturbances. For example, the ESO obtained in [25] couldn't accurately estimate the random disturbances, obviously. Thus, the disturbance-compensated performance of the obtained controller was decreased, greatly, when some random disturbances exist in the system. In order to deal with those complex disturbances, many researchers turned to using some nonlinear control strategies, such as sliding mode control(SMC), to improve the control performance of QUAVs. SMC is well known for its robustness in overcoming all types of disturbances and uncertainties appearing in the system. Moreover, the reaching time of the system to the sliding surface is finite and known [6], [26]. During the past several decades, some results about SMC for QUAVs have been obtained by many researchers. For example, an adaptive fractional-order SMC method for the QUAVs was proposed in [27]. As to those traditional SMC schemes, the error dynamics often fail to converge to zero in finite time. Thus, in order to decrease the influence of those system errors on system performance, many efforts have been made by scholars in recent years [28], [29], [30], [31]. In order to achieve a finite-time convergence of the error, a terminal sliding mode control (TSMC) scheme was given in [29]. Unfortunately, the TSMC could lead to a singularity problem in the control law. In order to solve this problem, a nonsingular terminal sliding mode control (NTSMC) was proposed in [30], which ensured that the system state converges quickly in a finite time. Nevertheless, due to the presence of symbolic functions in NTSMC, the control law might exhibit chattering and result in a decrease in the control accuracy [31].

However, for time-varying payloads, the traditional SMC may not satisfy the flying performance requirements of QUAVs. In order to solve this problem, an improved control technique, which combines the SMC with an adaptive control technology, was given in [32], and some improved performances were achieved. In [33], a new adaptive sliding mode control with finite-time convergence characteristics was proposed to guarantee quadrotor hovering in spite of parametric uncertainties and external disturbances. At the same time, by considering the complex flying surrounding of the QUAVs, an adaptive integral sliding mode control (ISMC) strategy for QUAVs was introduced in [34], which ensures fast and finite-time convergence of the system error along with a chattering attenuation. Moreover, some QUAVs' control schemes, which combined SMC with some other control techniques, were given by many scholars in the following years. For example, in [35], a control algorithm, which combined the integral sliding mode strategy with the backstepping technique, was proposed for the control of QUAVs with system uncertainties, and some improved results were achieved. In [36], a robust algorithm based on a fixed-time SMC was proposed for a QUAV, and some improved performances were achieved. Moreover, in [37], a fixed-time control strategy was presented to improve the transient response and robustness of a cable-suspended load with external disturbances. However, to the best of the authors' knowledge, as to the time-varying load and unknown disturbances for QUAVs, the existing achievements are relatively few, and obtaining some results in this field is still necessary and meaningful. This is the main motivation of this paper. In this paper, the ASMC and ARSMC cascaded controllers are designed for QUAVs with time-varying load and unknown disturbances. The time-varying load and unknown disturbances are estimated by the adaptive laws designed in the ASMC controller, which is used to control the position subsystem. Moreover, the unknown inner-loop disturbances are estimated by a self-turning law designed in the ARSMC controller, which is used to control the attitude subsystem. Furthermore, in order to reach the fast convergence and less chattering performances of the system, a NTSM combined with the recursive ISM is introduced in the design of the sliding mode surface. The main contributions of this paper are summarized as follows:

(1) A cascaded controller is designed to control QUAVs with time-varying loads and unknown disturbances to track the desired trajectory.

(2) the adaptive laws are formulated to estimate the upper bounds of time-varying loads and unknown disturbances appearing in the attitude and position subsystems.

(3) A recursive sliding mode controller is developed to guarantee the attitude tracking errors converge to zero in a finite time. Additionally, this controller incorporates an integral element to mitigate the chattering.

The remainder of this paper is organized as follows: The dynamic model of the QUAVs is presented in Section II. The control strategy is analyzed in Section III, where the ASMC and ARSMC are given. In Section IV, three simulations are presented to validate the effectiveness of the developed control scheme. The conclusions of this study and future work are given in Section V.

II. DYNAMIC MODEL OF QUAVS

As shown in Fig.2, the cross "×" shape QUAVs have four propellers. $\{O_e - x_e y_e z_e\}$ and $\{O_b - x_b y_b z_b\}$ are the space-fixed coordinate system and the body-fixed coordinate system of the QUAVs, respectively. The QUAVs achieve attitude control by four distinct drive propellers, and can be operated in six degrees of freedom in space [38]. Obviously, the QUAVs are multiple-input and multiple-output nonlinear systems. Therefore, to establish a general model for the QUAVs with time-varying loads, the following assumptions are proposed [39], [40], [41], [42], [43], [44], [45], and [46]:

Assumption 1: The quadrotor is a rigid body with a uniform mass distribution and center symmetry.

Assumption 2: The moment of inertia of a QUAV remains unchanged.

Assumption 3: The pulling force generated by the propeller on each wing of a QUAV is proportional to the speed of the motor.

According to the research results obtained in [36], [37], [38], [39], [40], [41], [42], and [43], the dynamic models of the QUAVs can be described as

$$\begin{cases} \ddot{x}_e = \frac{1}{m}\left(\cos\varphi\sin\theta\cos\psi + \sin\varphi\sin\psi\right)U_1 \\ \qquad -\frac{1}{m}k_x\dot{x}_e \\ \ddot{y}_e = \frac{1}{m}\left(\cos\varphi\sin\theta\sin\psi - \sin\varphi\cos\psi\right)U_1 \\ \qquad -\frac{1}{m}k_y\dot{y}_e \\ \ddot{z}_e = \frac{1}{m}\left(\cos\varphi\cos\theta\right)U_1 - \frac{1}{m}k_z\dot{z}_e - g \\ \ddot{\phi} = \frac{k_\phi d}{J_x}\dot{\phi} + \frac{U_2}{J_x} \\ \ddot{\theta} = \frac{k_\theta d}{J_y}\dot{\theta} + \frac{U_3}{J_y} \\ \ddot{\psi} = \frac{k_\psi d}{J_z}\dot{\psi} + \frac{U_4}{J_z} \end{cases} \tag{1}$$

where U_1, U_2, U_3 and U_4 represent the inputs applied to the altitude, roll, pitch and yaw channels, respectively. $\ddot{\phi}$, $\ddot{\theta}$ and $\ddot{\psi}$ are the accelerations of the roll, pitch, and yaw angles, respectively. $\ddot{x}$, $\ddot{y}$ and $\ddot{z}$ are the accelerations in the x, y and z-axis directions, respectively. Other variables are shown in the Table 1. The definitions of U_x, U_y and U_z are as followings.

$$\begin{cases} U_z = (\cos\varphi\cos\theta)U_1 \\ U_y = (\cos\varphi\sin\theta\sin\psi - \sin\varphi\cos\psi)U_1 \\ U_x = (\cos\varphi\sin\theta\cos\psi + \sin\varphi\sin\psi)U_1 \end{cases} \tag{2}$$

By doing a mathematic operation on (2), the descriptions of the desired angles can be expressed as

$$\begin{cases} \theta_d = \arctan\left(\frac{U_x\cos\psi + U_y\sin\psi}{U_z}\right) \\ \phi_d = \arctan\left(\cos\theta\frac{U_x\sin\psi - U_y\cos\psi}{U_z}\right) \\ U_1 = \frac{U_z}{\cos\theta_d\cos\phi_d} \end{cases} \tag{3}$$

Assume that the three directions(x, y and z) and three altitude angles (ϕ, θ and ψ) are all with unknown disturbances, which are expressed as $\Delta_j(j = x, y, z, \phi, \theta, \psi)$. According to the above-mentioned system(1), the QAUVs with unknown disturbances can be described as

$$\begin{cases} \ddot{x}_e = \frac{1}{m}\left(\cos\varphi\sin\theta\cos\psi + \sin\varphi\sin\psi\right)U_1 \\ \qquad -\frac{1}{m}k_x\dot{x}_e + \Delta_x \\ \ddot{y}_e = \frac{1}{m}\left(\cos\varphi\sin\theta\sin\psi - \sin\varphi\cos\psi\right)U_1 \\ \qquad -\frac{1}{m}k_y\dot{y}_e + \Delta_y \\ \ddot{z}_e = \frac{1}{m}\left(\cos\varphi\cos\theta\right)U_1 - \frac{1}{m}k_z\dot{z}_e \\ \qquad -g + \Delta_z \\ \ddot{\phi} = \frac{k_\phi d}{J_x}\dot{\phi} + \frac{U_2}{J_x} + \Delta_\phi \\ \ddot{\theta} = \frac{k_\theta d}{J_y}\dot{\theta} + \frac{U_3}{J_y} + \Delta_\theta \\ \ddot{\psi} = \frac{k_\psi d}{J_z}\dot{\psi} + \frac{U_4}{J_z} + \Delta_\psi \end{cases} \tag{4}$$

III. CONTROL STRATEGY

For the QUAVs described in (4), the ASMC and ARSMC cascaded controllers are designed such that the controlled QUAVs can track the desired trajectories. First, the desired inputs (x_d, y_d, z_d and ψ_d) are obtained by a signal emitter. Then, three ASMC controllers are designed to make the controlled QUAV track the desired trajectories (x_d, y_d and z_d). Moreover some adaptive laws are given to estimate the time-varying load and unknown disturbances. Second, an ARSMC controller is designed to guarantee the controlled angles tracking those desired angles. Based on the control requirements, the control scheme, shown in Fig. 1, is obtained. Moreover, a tracking differentiator (TD), which is shown in (3), is used to obtain the first and second derivatives of the input signal [47].

$$\begin{cases} \dot{x}_1 = x_2 \\ \dot{x}_2 = x_3 \\ \varepsilon^3\dot{x}_3 = -2^{3/5}4(x_1 - v(t) + (\varepsilon x_2)^{9/7})^{1/3} \\ \qquad -4(\varepsilon^3 x_3)^{3/5} \end{cases} \tag{5}$$

where $\varepsilon = 0.04$; $v(t)$ is an input signal; x_1 is the tracking of the input signal; x_2 is the estimation of the first derivative of the input signal, and x_3 is the estimation of the second derivative of the input signal.

A. ARSMC CONTROLLER FOR ATTITUDE SUBSYSTEM

Based on (4), the dynamic model of ϕ, θ and ψ can be written as

$$\begin{cases} \ddot{\phi} = \frac{k_\phi d}{J_x}\dot{\phi} + \frac{U_2}{J_x} + \Delta_\phi \\ \ddot{\theta} = \frac{k_\theta d}{J_y}\dot{\theta} + \frac{U_3}{J_y} + \Delta_\theta \\ \ddot{\psi} = \frac{k_\psi d}{J_z}\dot{\psi} + \frac{U_4}{J_z} + \Delta_\psi \end{cases} \tag{6}$$

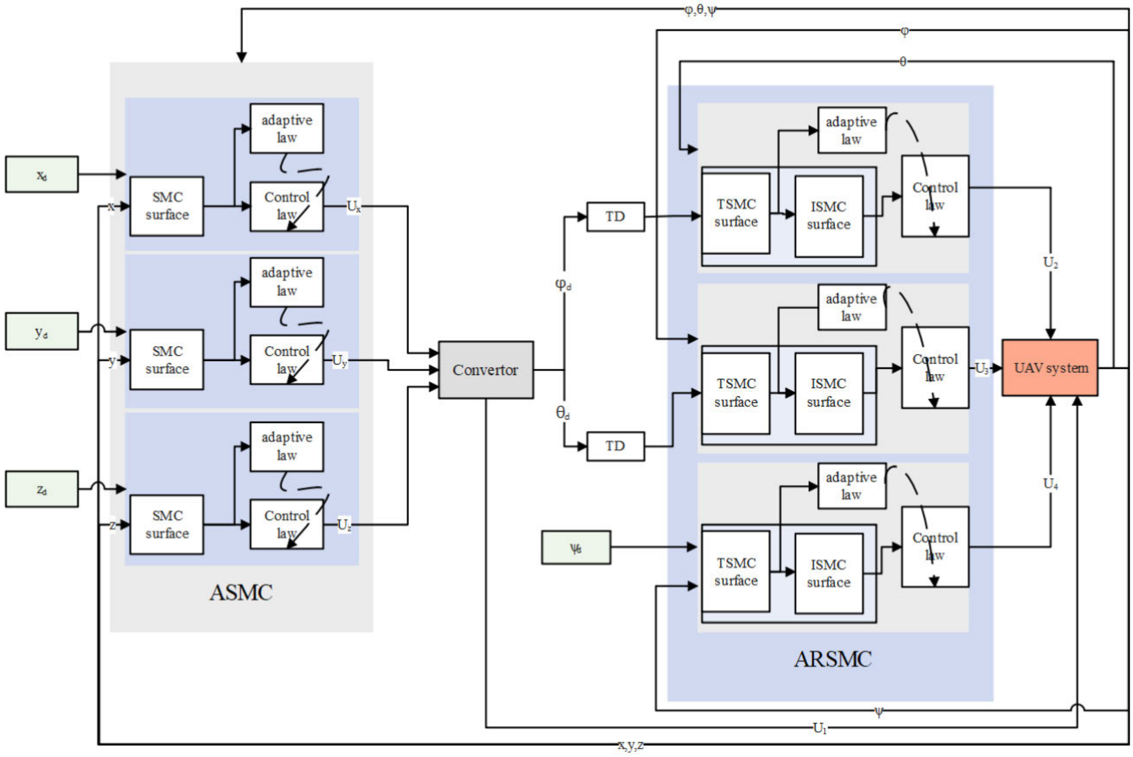

FIGURE 1. Control scheme.

where, Δ_ϕ, Δ_θ and Δ_ψ represent the unknown disturbances within the three angle channels (ϕ, θ and ψ), respectively, and their upper bounds can be expressed as [48]

$$\begin{cases} \Delta_\phi \le b_{\phi 0} + b_{\phi 1}\left|e_\phi\right| + b_{\phi 2}\left|\dot{e}_\phi\right| \\ \Delta_\theta \le b_{\theta 0} + b_{\theta 1}\left|e_\theta\right| + b_{\theta 2}\left|\dot{e}_\theta\right| \\ \Delta_\psi \le b_{\psi 0} + b_{\psi 1}\left|e_\psi\right| + b_{\psi 2}\left|\dot{e}_\psi\right| \end{cases} \tag{7}$$

where b_{i0}, b_{i1} and $b_{i2}(i{=}\phi, \theta, \psi)$ are all positive numbers. Then, the state errors can be defined as

$$\begin{cases} e_\phi = \phi - \phi_d \\ e_\theta = \theta - \theta_d \\ e_\psi = \psi - \psi_d \\ \dot{e}_\phi = \dot{\phi} - \dot{\phi}_d \\ \dot{e}_\theta = \dot{\theta} - \dot{\theta}_d \\ \dot{e}_\psi = \dot{\psi} - \dot{\psi}_d \end{cases} \tag{8}$$

where ϕ_d, θ_d and ψ_d are the desired attitude angles.

From Fig.1, it can be seen that ARSMC has two recursive surfaces: a NTSM and an ISM. Compared with some other sliding mode manifolds, the NTSM has finite-time convergence speed when the state are far from the origin [49], and the ISM also can decrease the chattering.

The NTSM is chosen as the following [50]:

$$\begin{cases} \varepsilon_\phi = e_\phi + \lambda_\phi\left|\dot{e}_\phi\right|^{\alpha_\phi} sign(\dot{e}_\phi) \\ \varepsilon_\theta = e_\theta + \lambda_\theta\left|\dot{e}_\theta\right|^{\alpha_\theta} sign(\dot{e}_\theta) \\ \varepsilon_\psi = e_\psi + \lambda_\psi\left|\dot{e}_\psi\right|^{\alpha_\psi} sign(\dot{e}_\psi) \end{cases} \tag{9}$$

where $\lambda_i(i{=}\phi, \theta, \psi)$ are positive constants; $\alpha_i{>}1(i{=}\phi, \theta, \psi)$ are the division of two positive odd numbers. Under the initial conditions of $e(0)_i = 0$ and $\dot{e}(0)_i = 0$, it can be gotten that the system is converged to zero in the finite time t_{ei}, which satisfies [51].

$$t_{ei} = \frac{\lambda_i^{-(1/\alpha_i)}}{1-(1/\alpha_i)} \tag{10}$$

The recursive integral terminal sliding surfaces are proposed as the following [52]

$$\begin{cases} s_\phi = \varepsilon_\phi + \omega_\phi\sigma_\phi \\ s_\theta = \varepsilon_\theta + \omega_\theta\sigma_\theta \\ s_\psi = \varepsilon_\psi + \omega_\psi\sigma_\psi \end{cases} \tag{11}$$

where $\omega_i > 0$. $\dot{\sigma}_i$ ($i{=}\phi, \theta$ and ψ) are given by

$$\begin{cases} \dot{\sigma}_\phi = \left|\varepsilon_\phi\right|^{\beta_\phi} sign(\varepsilon_\phi) \\ \dot{\sigma}_\theta = \left|\varepsilon_\theta\right|^{\beta_\theta} sign(\varepsilon_\theta) \\ \dot{\sigma}_\psi = \left|\varepsilon_\psi\right|^{\beta_\psi} sign(\varepsilon_\psi) \end{cases} \tag{12}$$

where $0 < \beta_i < 1$, $i{=}\phi$, θ and ψ, respectively. The initial values of σ_i are designed as

$$\sigma_i(0) = -\frac{\varepsilon_i(0)}{\omega_i} \tag{13}$$

Then, it can be gotten that $s_i(0) = 0$. The attitude angles and angular velocities can be measured by the sensors. Then the

$\varepsilon_i(0)$ (i=ϕ, θ and ψ) are calculated by

$$\begin{cases} \varepsilon_\phi(0) = \omega_\phi^{-1}(e_\phi(0) + \lambda_\phi \left|\dot{e}_\phi(0)\right|^{\alpha_\phi} sign(\dot{e}_\phi(0))) \\ \varepsilon_\theta(0) = \omega_\theta^{-1}(e_\theta(0) + \lambda_\theta \left|\dot{e}_\theta(0)\right|^{\alpha_\theta} sign(\dot{e}_\theta(0))) \\ \varepsilon_\psi(0) = \omega_\psi^{-1}(e_\psi(0) + \lambda_\psi \left|\dot{e}_\psi(0)\right|^{\alpha_\psi} sign(\dot{e}_\psi(0))) \end{cases} \tag{14}$$

then $s_i(0) = 0$ (i=ϕ, θ and ψ). By simplifying and integrating (12), it yields

$$\int_0^{t_{\varepsilon i}} \frac{|\varepsilon_i|^{-\beta_i}}{\omega_i} d|\varepsilon_i| = \int_0^{t_{\varepsilon i}} d|t| \tag{15}$$

Then, it gets [53]:

$$t_{\varepsilon i} = \frac{|\varepsilon_i(0)|^{1-\beta_i}}{\omega_i(1-\beta_i)} \tag{16}$$

By applying derivative on sliding surface s_i in (11) and considering (12), we can obtain

$$\begin{cases} \dot{s}_i = \dot{\varepsilon}_i + \omega_i\dot{\sigma}_i \\ = \dot{e}_i + \lambda_i\alpha_i|\dot{e}_i|^{\alpha_i-1}\ddot{e}_i + \omega_i\dot{\sigma}_i \\ = \dot{e}_i + \lambda_i\alpha_i|\dot{e}_i|^{\alpha_i-1}(\ddot{i} - \ddot{i}_d) + \omega_i\dot{\sigma}_i \end{cases} \tag{17}$$

When $\dot{s}_i = 0$ and $\Delta_i = 0$, by considering the subsystem (6) and (17), we can obtain

$$U_{eqi} = \frac{|\dot{e}_i|^{1-\alpha_i} J_i}{\lambda_i\alpha_i}(-\dot{e}_i - \omega_i\dot{\sigma}_i) + dk_i\dot{i} + \ddot{i}_d J_i \tag{18}$$

where $J_\phi = J_x$, $J_\theta = J_y$ and $J_\psi = J_z$. To enhance the controller's anti-disturbance performance, the switching control laws can be designed as

$$U_{swi} = -\frac{|\dot{e}_i|^{1-\alpha_i} J_i}{\lambda_i\alpha_i}(k_{i1}s_i + k_{i2}\left|s_i\right|^v sign(s_i) + (\hat{b}_{i0} + \hat{b}_{i1}\left|e_i\right| + \hat{b}_{i2}\left|\dot{e}_i\right|)sign(s_i)) \tag{19}$$

where $0 < v < 1$. Both k_{i1} and k_{i2} are positive constants. The estimations of b_{i0}, b_{i1} and b_{i2} are denoted as $\hat{b}_{i0}$, $\hat{b}_{i1}$ and $\hat{b}_{i2}$, respectively, and the adaptive laws of b_{i0}, b_{i1} and b_{i2} can be described as

$$\begin{cases} \dot{\hat{b}}_{i0} = \eta_{i0}\left|s_i\right| \\ \dot{\hat{b}}_{i1} = \eta_{i1}\left|e_i\right|\left|s_i\right| \\ \dot{\hat{b}}_{i2} = \eta_{i2}\left|\dot{e}_i\right|\left|s_i\right| \end{cases} \tag{20}$$

where η_{i0}, η_{i1} and η_{i2} are all positive constants. Then, the control law for quadrotor attitude subsystem can be written as

$$\begin{cases} U_2 = U_{eq\phi} + U_{sw\phi} \\ U_3 = U_{eq\theta} + U_{sw\theta} \\ U_4 = U_{eq\psi} + U_{sw\psi} \end{cases} \tag{21}$$

Moreover, the adaptive estimation errors are defined as

$$\begin{cases} \widetilde{b}_{i0} = b_{i0} - \hat{b}_{i0} \\ \widetilde{b}_{i1} = b_{i1} - \hat{b}_{i1} \\ \widetilde{b}_{i2} = b_{i2} - \hat{b}_{i2} \end{cases} \tag{22}$$

Lemma 1 [43]: considering the attitude subsystem(6) with the upper bounds of unknown disturbances(7) and the designed adaptive laws(20), there exist $b_{\phi i}$, $b_{\theta i}$ and $b_{\psi i}$ in (7) such that $\widetilde{b}_{i0} \le 0$, $\widetilde{b}_{i1} \le 0$ and $\widetilde{b}_{i2} \le 0$, where $\widetilde{b}_{ij}(j = 0, 1, 2)$ are shown in (22).

Then, let's come to proof the finite-time convergence of the ARSMC. Define the Lyapunov function as follows.

$$V = \frac{1}{2}s_z s_z + \frac{1}{2}p_{i0}\widetilde{b}_{i0}^2 + \frac{1}{2}p_{i1}\widetilde{b}_{i1}^2 + \frac{1}{2}p_{i2}\widetilde{b}_{i2}^2 \tag{23}$$

By substituting $\dot{s}_i$ and (6) into the time derivative of (23), it yields:

$$\begin{aligned} \dot{V} &= s_i\dot{s}_i + p_{i0}\widetilde{b}_{i0}\dot{\widetilde{b}}_{i0} + +p_{i1}\widetilde{b}_{i1}\dot{\widetilde{b}}_{i1} + p_{i2}\widetilde{b}_{i2}\dot{\widetilde{b}}_{i2} \\ &= s_i(\dot{e}_i + \lambda_i\alpha_i|\dot{e}_i|^{\alpha_i-1}(\ddot{i} - \ddot{i}_d) + \omega_i\dot{\sigma}_i) \\ &\quad + p_{i0}\widetilde{b}_{i0}\dot{\widetilde{b}}_{i0} + p_{i1}\widetilde{b}_{i1}\dot{\widetilde{b}}_{i1} + p_{i2}\widetilde{b}_{i2}\dot{\widetilde{b}}_{i2} \\ &= s_i(\lambda_i\alpha_i|\dot{e}_i|^{\alpha_i-1}(\frac{k_i d}{J_i}\dot{i} + \frac{U_{eqi} + U_{swi}}{J_i} \\ &\quad + \Delta_i - \ddot{i}_d) + \dot{e}_i + \omega_i\dot{\sigma}_i) + p_{i0}\widetilde{b}_{i0}\dot{\widetilde{b}}_{i0} \\ &\quad + p_{i1}\widetilde{b}_{i1}\dot{\widetilde{b}}_{i1} + p_{i2}\widetilde{b}_{i2}\dot{\widetilde{b}}_{i2} \end{aligned} \tag{24}$$

By substituting the equivalent control laws (18) and the switching control laws (19) into (24), we can obtain.

$$\begin{aligned} \dot{V} &= s_i(-k_{i1}s_i - k_i2\left|s_i\right|^v sign(s_i) - \Delta_i \\ &\quad - (\hat{b}_{i0} + \hat{b}_{i1}\left|e_i\right| + \hat{b}_{i2}\left|\dot{e}_i\right|)sign(s_i)) \\ &\quad + \dot{e}_i + \omega_i\dot{\sigma}_i) + p_{i0}\widetilde{b}_{i0}\dot{\widetilde{b}}_{i0} + p_{i1}\widetilde{b}_{i1}\dot{\widetilde{b}}_{i1} + p_{i2}\widetilde{b}_{i2}\dot{\widetilde{b}}_{i2} \\ &= (-k_{i1}s_is_i - k_i2\left|s_i\right|^{v+1} - \Delta_i s_i \\ &\quad - (\hat{b}_{i0} + \hat{b}_{i1}\left|e_i\right| + \hat{b}_{i2}\left|\dot{e}_i\right|)\left|s_i\right|) \\ &\quad + \dot{e}_i + \omega_i\dot{\sigma}_i) + p_{i0}\widetilde{b}_{i0}\dot{\widetilde{b}}_{i0} + p_{i1}\widetilde{b}_{i1}\dot{\widetilde{b}}_{i1} + p_{i2}\widetilde{b}_{i2}\dot{\widetilde{b}}_{i2} \\ &\le (-k_{i1}s_is_i - k_i2\left|s_i\right|^{v+1} - \left|\Delta_i\right|\left|s_i\right| \\ &\quad - (\hat{b}_{i0} + \hat{b}_{i1}\left|e_i\right| + \hat{b}_{i2}\left|\dot{e}_i\right|)\left|s_i\right|) \\ &\quad + \dot{e}_i + \omega_i\dot{\sigma}_i) + p_{i0}\widetilde{b}_{i0}\dot{\widetilde{b}}_{i0} + p_{i1}\widetilde{b}_{i1}\dot{\widetilde{b}}_{i1} + p_{i2}\widetilde{b}_{i2}\dot{\widetilde{b}}_{i2} \\ &\le -(\hat{b}_{i0} + \hat{b}_{i1}\left|e_i\right| + \hat{b}_{i2}\left|\dot{e}_i\right|)\left|s_i\right| + \left|\Delta_i\right|\left|s_i\right| \\ &\quad + p_{i0}\widetilde{b}_{i0}\dot{\widetilde{b}}_{i0} + p_{i1}\widetilde{b}_{i1}\dot{\widetilde{b}}_{i1} + p_{i2}\widetilde{b}_{i2}\dot{\widetilde{b}}_{i2} \end{aligned} \tag{25}$$

Based on the adaptive laws (20), we can obtain that $\dot{V}$ satisfies

$$\begin{aligned} \dot{V} &\le -(\hat{b}_{i0} + \hat{b}_{i1}\left|e_i\right| + \hat{b}_{i2}\left|\dot{e}_i\right|)\left|s_i\right| + \left|\Delta_i\right|\left|s_i\right| \\ &\quad + (p_{i0}\eta_{i0} - 1)\widetilde{b}_{i0}\left|s_i\right| + (p_{i1}\eta_{i1} - 1)\widetilde{b}_{i1}\left|e_i\right|\left|s_i\right| \\ &\quad + (p_{i2}\eta_{i2} - 1)\widetilde{b}_{i2}\left|\dot{e}_i\right|\left|s_i\right| \end{aligned} \tag{26}$$

Based on Lemma 1, we can obtain $\widetilde{b}_{i0} \le 0$, $\widetilde{b}_{i1} \le 0$ and $\widetilde{b}_{i2} \le 0$, and then, it yields

$$\begin{aligned} \dot{V} &\le -(\hat{b}_{i0} + \hat{b}_{i1}\left|e_i\right| + \hat{b}_{i2}\left|\dot{e}_i\right|)\left|s_i\right| + \left|\Delta_i\right|\left|s_i\right| \\ &\quad - (p_{i0}\eta_{i0} - 1)\left|\widetilde{b}_{i0}\right|\left|s_i\right| - (p_{i1}\eta_{i1} - 1)\left|\widetilde{b}_{i1}\right|\left|e_i\right|\left|s_i\right| \\ &\quad - (p_{i2}\eta_{i2} - 1)\left|\widetilde{b}_{i2}\right|\left|\dot{e}_i\right|\left|s_i\right| \end{aligned} \tag{27}$$

Define the following variables.

$$\begin{aligned} c_i &= (\hat{b}_{i0} + \hat{b}_{i1}|e_i| + \hat{b}_{i2}|\dot{e}_i| - |\Delta_i|) \\ c_{i0} &= (p_{i0}\eta_{i0} - 1)|s_i| \\ c_{i1} &= (p_{i1}\eta_{i1} - 1)|e_i||s_i| \\ c_{i2} &= (p_{i2}\eta_{i2} - 1)|\dot{e}_i||s_i| \end{aligned} \tag{28}$$

Then, we have

$$\begin{aligned} \dot{V} &\leq -c_i|s_i| - c_{i0}|\widetilde{b}_{i0}| - c_{i1}|\widetilde{b}_{i1}| - c_{i2}|\widetilde{b}_{i2}| \\ &\leq -c_i\sqrt{2}\sqrt{\frac{1}{2}}|s_i| - c_{i0}\sqrt{2p_{i0}^{-1}}\sqrt{\frac{p_{i0}}{2}}|\widetilde{b}_{i0}| \\ &\quad - c_{i1}\sqrt{2p_{i1}^{-1}}\sqrt{\frac{p_{i1}}{2}}|\widetilde{b}_{i1}| - c_{i2}\sqrt{2p_{i2}^{-1}}\sqrt{\frac{p_{i2}}{2}}|\widetilde{b}_{i2}| \\ &\leq -k(\sqrt{\frac{1}{2}}|s_i| + \sqrt{\frac{p_{i0}}{2}}|\widetilde{b}_{i0}| + \sqrt{\frac{p_{i1}}{2}}|\widetilde{b}_{i1}| \\ &\quad + \sqrt{\frac{p_{i2}}{2}}|\widetilde{b}_{i2}|) \end{aligned} \tag{29}$$

where $k = min(c_i\sqrt{2}, c_{i0}\sqrt{2p_{i0}^{-1}}, c_{i1}\sqrt{2p_{i1}^{-1}}, c_{i2}\sqrt{2p_{i2}^{-1}}) > 0$. Then, based on (23), it yields

$$\begin{aligned} V^{\frac{1}{2}} &= \sqrt{\frac{1}{2}s_z s_z + \frac{1}{2}p_{i0}\widetilde{b}_{i0}^2 + \frac{1}{2}p_{i1}\widetilde{b}_{i1}^2 + \frac{1}{2}p_{i2}\widetilde{b}_{i2}^2} \\ &\leq \sqrt{\frac{1}{2}s_z s_z} + \sqrt{\frac{1}{2}p_{i0}\widetilde{b}_{i0}^2} + \sqrt{\frac{1}{2}p_{i1}\widetilde{b}_{i1}^2} + \sqrt{\frac{1}{2}p_{i2}\widetilde{b}_{i2}^2} \\ &\leq (\sqrt{\frac{1}{2}}|s_i| + \sqrt{\frac{p_{i0}}{2}}|\widetilde{b}_{i0}|\sqrt{\frac{p_{i1}}{2}}|\widetilde{b}_{i1}| + \sqrt{\frac{p_{i2}}{2}}|\widetilde{b}_{i2}|) \end{aligned} \tag{30}$$

According to (29) and (30), the relationship between $\dot{V}$ and V satisfies

$$\dot{V} \leq -kV^{\frac{1}{2}} \tag{31}$$

Then, it is easy to obtain that V converges to zero in a finite time, and t_v satisfies

$$t_v \leq \frac{2V(0)^{\frac{1}{2}}}{k} \tag{32}$$

Therefore, the tracking error converge to zero in a finite time $(t_{ei} + t_{\epsilon i} + t_v)$. ■

Theorem 1: Considering the attitude subsystem(6), the controller(21) guarantees the attitude tracking error converges to zero in a finite time.

Remark 1: In order to achieve the satisfying controlling results, a rule for choosing those parameters in the controller design is summarized as follows:the positive constants λ_i (i=ϕ, θ, ψ) and α_i (i=ϕ, θ, ψ) in (9) should not be chosen to be too large numbers, and the values of them can be adjusted for searching a better controlling result. Moreover, The constant variables in (11) and (12) conform to: $\omega_i > 0$ (i=ϕ, θ, ψ) and $0 < \beta_i < 1$ (i=ϕ, θ, ψ). The values of ω_i (i=ϕ, θ, ψ) should not be too large, otherwise, the convergence time obtained in (16) will be long, and the gain of the obtained controller in (21) will be high. The parameters used to obtain the attitude controller in this paper are given in table 2.

B. ASMC CONTROLLER FOR POSITION SUBSYSTEM

Based on (4), the position subsystems of the QUAVs can be expressed as

$$\begin{cases} \ddot{x}_e = \frac{1}{m}(\cos\varphi\sin\theta\cos\psi + \sin\varphi\sin\psi)U_1 \\ \quad -\frac{1}{m}K_x\dot{x}_e + \Delta_x \\ \ddot{y}_e = \frac{1}{m}(\cos\varphi\sin\theta\sin\psi - \sin\varphi\cos\psi)U_1 \\ \quad -\frac{1}{m}K_y\dot{y}_e + \Delta_y \\ \ddot{z}_e = \frac{1}{m}(\cos\varphi\cos\theta)U_1 - \frac{1}{m}K_x\dot{z}_e - g + \Delta_z \end{cases} \tag{33}$$

where Δ_x, Δ_y and Δ_z, which are the unknown bounded disturbances, satisfy

$$\begin{cases} |\Delta_x| \leq \alpha_x \\ |\Delta_y| \leq \alpha_y \\ |\Delta_z| \leq \alpha_z \end{cases} \tag{34}$$

where α_x, α_y and α_z are unknown positive constants. Define the tracking errors as

$$\begin{cases} e_x = x - x_d \\ e_y = y - y_d \\ e_z = z - z_d \\ \dot{e}_x = \dot{x} - \dot{x}_d \\ \dot{e}_y = \dot{y} - \dot{y}_d \\ \dot{e}_z = \dot{z} - \dot{z}_d \end{cases} \tag{35}$$

Then, consider the sliding mode surfaces as

$$\begin{cases} s_x = \dot{e}_x + r_x e_x \\ s_y = \dot{e}_y + r_y e_y \\ s_z = \dot{e}_z + r_z e_z \end{cases} \tag{36}$$

By taking the time derivative on the sliding mode surfaces, we have

$$\begin{cases} \dot{s}_x = \ddot{e}_x + r_x\dot{e}_x \\ \dot{s}_y = \ddot{e}_x + r_y\dot{e}_y \\ \dot{s}_z = \ddot{e}_x + r_z\dot{e}_z \end{cases} \tag{37}$$

The self-turning law can be designed as

$$\begin{cases} \dot{\hat{\Delta}}_x = \beta_{x1}|s_y| \\ \dot{\hat{\Delta}}_y = \beta_{y1}|s_y| \\ \dot{\hat{\Delta}}_z = \beta_{z1}|s_z| \\ \dot{\hat{m}} = -\beta_{z2}{s_z}^T(g + \ddot{z}_d - k_z\dot{e} - c_1 s_z) \end{cases} \tag{38}$$

Then, in the z-axis control channel, the control law can be designed as

$$\begin{aligned} \dot{s}_z &= \ddot{z} - \ddot{z}_d + k_z\ddot{\varepsilon}_z \\ &= \frac{1}{m}(\cos\varphi\cos\theta)U_1 - \frac{1}{m}K_{flx}\dot{z}_e \\ &\quad -g - \ddot{z}_d + k_z\ddot{\varepsilon}_z \\ &= \frac{U_a + \Delta_z}{m} - g - \ddot{z}_d + k_z\ddot{\varepsilon}_z \end{aligned} \tag{39}$$

where $U_a = (\cos\varphi\cos\theta)\,U_1 - K_{flx}\dot{z}_e$ is a virtual control input. U_a is designed as

$$\begin{cases} U_a = \hat{m}\bar{U}_a - \hat{\Delta}_z \\ \bar{U}_a = g + \ddot{z}_d - k_z\dot{e} - c_1 s_z \end{cases} \tag{40}$$

where $c_1 > 0$; $\hat{m}$ and $\hat{\Delta}_z$ are the estimations of the mass and the total disturbances, respectively. By substituting (38) into (39), it is obtained that

$$\begin{aligned} \dot{s}_z &= \frac{U_a + \Delta_z}{m} - g - \ddot{z}_d + k_z\ddot{e}_z \\ &= \frac{\hat{m}\bar{U}_a - \hat{\Delta}_z + \Delta_z}{m} - g - \ddot{z}_d + k_z\ddot{e}_z \end{aligned} \tag{41}$$

Now, define the estimation errors of mass and unknown disturbances as $\tilde{m}$, $\tilde{\Delta}_x$, $\tilde{\Delta}_y$ and $\tilde{\Delta}_z$, which satisfy

$$\begin{cases} \tilde{\Delta}_x = \Delta_x - \hat{\Delta}_x \\ \tilde{\Delta}_y = \Delta_y - \hat{\Delta}_y \\ \tilde{\Delta}_z = \Delta_z - \hat{\Delta}_z \\ \tilde{m}_z = m - \hat{m} \end{cases} \tag{42}$$

By taking the time derivative on (42), we can obtain

$$\begin{cases} \dot{\tilde{\Delta}}_x = -\dot{\hat{\Delta}}_x \\ \dot{\tilde{\Delta}}_y = -\dot{\hat{\Delta}}_y \\ \dot{\tilde{\Delta}}_z = -\dot{\hat{\Delta}}_z \\ \dot{\tilde{m}} = -\dot{\hat{m}} \end{cases} \tag{43}$$

Consider the following Lyapunov function candidate:

$$V = \frac{1}{2}m{s_z}^T s_z + \frac{1}{2\beta_{z1}}\tilde{\Delta}_z^T\tilde{\Delta}_z + \frac{1}{2\beta_{z2}}\tilde{m}^2 \tag{44}$$

By doing a time derivative on V, we can obtain

$$\dot{V} = m{s_z}^T\dot{s}_z + \frac{1}{\beta_{z1}}\tilde{\Delta}_z^T\dot{\tilde{\Delta}}_z + \frac{1}{\beta_{z2}}\tilde{m}\dot{\tilde{m}} \tag{45}$$

Then, by substituting (39) and (40) into (45), it yields

$$\begin{aligned} \dot{V} &= m{s_z}^T\left(\frac{\hat{m}\bar{U}_a - \hat{\Delta}_z + \Delta_z}{m} - \bar{U}_a - c_1 s_z\right) \\ &\quad + \frac{1}{\beta_{z1}}\tilde{\Delta}_z^T\dot{\tilde{\Delta}}_z + \frac{1}{\beta_{z2}}\tilde{m}\dot{\tilde{m}} \\ &= \hat{m}\bar{U}_a{s_z}^T - \hat{\Delta}_z{s_z}^T + \Delta_z s^T - m{s_z}^T\bar{U}_a \\ &\quad - mc_1 s^T s_z + \frac{1}{\beta_{z1}}\tilde{\Delta}_z^T\dot{\tilde{\Delta}}_z + \frac{1}{\beta_{z2}}\tilde{m}\dot{\tilde{m}} \\ &= \; -\tilde{m}\bar{U}_a{s_z}^T + \tilde{\Delta}_z{s_z}^T - c_1{s_z}^T s_z \\ &\quad - \frac{1}{\beta_{z1}}\tilde{\Delta}_z^T\dot{\tilde{\Delta}}_z + \frac{1}{\beta_{z2}}\tilde{m}\dot{\tilde{m}} \end{aligned} \tag{46}$$

By substituting (43) and (38) into (46), one gets

$$\begin{aligned} \dot{V} &= -\tilde{m}\bar{U}_a{s_z}^T + \tilde{\Delta}_z{s_z}^T - c_1{s_z}^T s_z \\ &\quad - \frac{1}{\beta_{z1}}\tilde{\Delta}_z^T\dot{\hat{\Delta}}_z + \frac{1}{\beta_{z2}}\tilde{m}(-\dot{\hat{m}}) \\ &= -c_1{s_z}^T s_z - \frac{1}{\beta_{z1}}\tilde{\Delta}_z^T(\dot{\hat{\Delta}}_z - \beta_{z1}s_z) \\ &\quad - \frac{1}{\beta_{z2}}\tilde{m}(\dot{\hat{m}} + \beta_{z2}{s_z}^T\bar{U}_a) \\ &\le -c_1{s_z}^T s_z \le 0 \end{aligned} \tag{47}$$

Thus, when $s_z \neq 0$, we can get $\dot{V} < 0$, that is, s_z, $\tilde{\Delta}_z$ and $\tilde{m}$ are all gradually convergent. ■

The operations for obtaining the control laws in x and y-axis channels have the similar processes as those in z-axis channel. The control laws in x and y-axis channels can be expressed as

$$\begin{cases} U_b = \hat{m}\bar{U}_b - \hat{\Delta}_x \\ \bar{U}_b = \ddot{x}_d - k_x\dot{e} - c_1 s_x \\ U_c = \hat{m}\bar{U}_c - \hat{\Delta}_y \\ \bar{U}_c = \ddot{y}_d - k_y\dot{e} - c_1 s_y \end{cases} \tag{48}$$

where U_b and U_c are the control laws in x and y-axis channels, respectively.

Remark 2: It is worth mentioning that the trajectory tracking in the space-fixed coordinate system depends on the attitude adjustment in the body-fixed coordinate system. Thus, the controller design of QUAVs is divided into two parts:the attitude controller design and the position controller design. Accordingly, the part III is divided into two parts: part A and B. Part A concerns the controller design for attitude subsystem; Part B concerns the controller design for position subsystem.

IV. SIMULATION RESULTS AND ANALYSIS

In this section, three different kinds of trajectories are used to verify the performance of the proposed control strategy for the QAUVs under the time-varying load and unknown disturbances. The parameters of the considered QUAV are listed in Table1; the parameters of the controller are shown in the Table2; and the unknown disturbances within the six channels are shown in Fig.3. Then, three cases (see the following case 1-3) are used to perform the simulations; they all have the same initial value of $m = 2$ kg; and the desired yaw angles in the three cases satisfy $\psi_d = \pi/6$.

Case 1: This case is designed to imitate the agricultural sowing process, which has the time-varying load shown in (49). The initial value $m = 2$ kg within the first 5 seconds, then the sowing starts and lasts till the 25th second, and then, the QUAV returns back to the starting point from the 25th second to the 30th second.

$$m = \begin{cases} 2, & 0 \le t < 5 \\ 2 - 0.05(t-5), & 5 \le t < 25 \\ 1, & 25 \le t \end{cases} \tag{49}$$

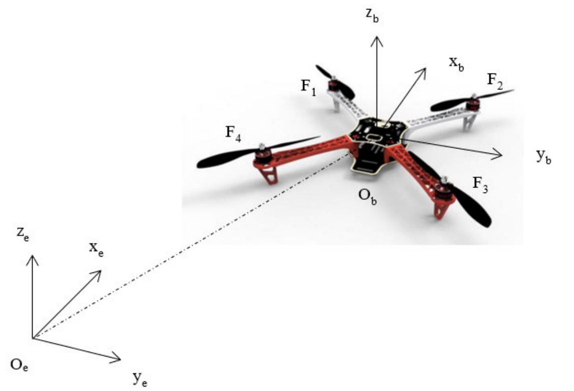

FIGURE 2. Schematic diagram of the quadrotor shape and coordinate system.

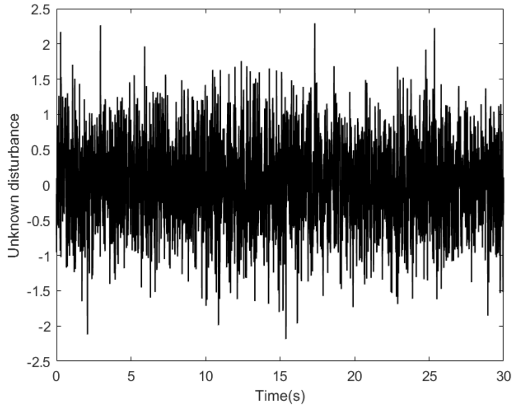

FIGURE 3. The signal of the unknown disturbances.

TABLE 1. The parameters of the QUAV.

Symbol	Meaning	Value and Units
J_x	Inertial moment along x axis	$4\times10^{-3}(N\cdot m/rad/s^2)$
J_y	Inertial moment along y axis	$4\times10^{-3}(N\cdot m/rad/s^2)$
J_z	Inertial moment along z axis	$8\times10^{-3}(N\cdot m/rad/s^2)$
d	Arm length of quadrotor	$0.25(m)$
k_x	Translation drag coefficient	$5\times10^{-4}(N/m/s)$
k_y	Translation drag coefficient	$5\times10^{-4}(N/m/s)$
k_z	Translation drag coefficient	$6\times10^{-4}(N/m/s)$
k_ϕ	Rotation Drag coefficient	$5\times10^{-4}(N\cdot m/rad/s)$
k_θ	Rotation Drag coefficient	$5\times10^{-4}(N\cdot m/rad/s)$
k_ψ	Translation drag coefficient	$6\times10^{-4}(N/m/s)$
m	Mass of quadrotor UAV	$2(kg)$
g	Acceleration of gravity	$9.8(m/s^2)$

TABLE 2. Controller parameters of UAV.

ASM	$ARSM$	$ARSMC$	$ARSMC$
$c_1=6$	$\lambda_\phi=0.5$	$\lambda_\theta=0.5$	$\lambda_\psi=0.9$
$\beta_{z2}=0.25$	$\alpha_\phi=7/5$	$\alpha_\theta=7/5$	$\alpha_\psi=7/5$
$\beta_{y2}=0.25$	$\beta_\phi=0.5$	$\beta_\theta=0.5$	$\beta_\psi=0.1$
$\beta_{x2}=0.25$	$\omega_\phi=0.5$	$\omega_\theta=0.5$	$\omega_\psi=0.1$
$\beta_{x2}=0.25$	$k_{\phi1}=0.5$	$k_{\theta1}=0.5$	$k_{\psi1}=0.5$
$\beta_{z1}=0.5$	$k_{\phi2}=0.5$	$k_{\theta2}=0.5$	$k_{\psi2}=0.5$
$\beta_{y1}=0.5$	$\upsilon_{\phi2}=0.8$	$\upsilon_{\theta2}=0.8$	$\upsilon_{\psi2}=0.8$
$\beta_{x1}=0.5$	$\eta_{\phi0}=0.5$	$\eta_{\theta0}=0.5$	$\eta_{\psi0}=0.1$
$r_z=0.1$	$\eta_{\phi1}=0.5$	$\eta_{\theta1}=0.5$	$\eta_{\psi1}=0.1$
$r_x=r_y=0.005$	$\eta_{\phi2}=0.5$	$\eta_{\theta2}=0.5$	$\eta_{\psi2}=0.1$

The desired trajectory is as following:

$$\begin{cases} x_d = \frac{1}{5}\cos(\frac{t}{4}) \\ y_d = \frac{1}{5}\sin(\frac{t}{8}) \\ z_d = \frac{1}{2} + 0.4\sin(t) \end{cases} \tag{50}$$

After finishing the simulations by computers, the flying results are obtained, and shown in the Figs.4-7. Fig.4 gives the 3D results of the trajectory tracking. Fig.5 is the tracking error of x, y and z. Fig.6 is the tracking error of ϕ, θ and ψ. The estimation error of m is given in Fig.7. Fig.4 shows that the controlled QUNV can successfully track the desired trajectory. From Fig.5-6, we can obtain, both the position and angle can be tracked quickly. Moreover, when the QUNV succeeds in tracking the desired trajectory, the maximum position tracking error is only 0.02 m. the maximum angle tracking error is only 0.03 deg. Fig.7 shows, although the system is disturbed by some unknown signals, the mass can still be estimated successfully, and the estimating error is less than 0.08 kg, which is 8% of the whole mass.

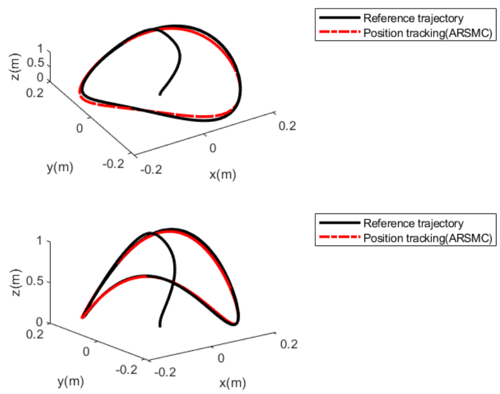

FIGURE 4. The 3D trajectory tracking results in case 1.

Case 2: This case is designed to imitate the act of dropping supplies, which has the time-varying load satisfying (51). The initial value $m = 2$ kg within the first 10 seconds, then the first time dropping action happens at the 10th second, and the second time dropping action happens at the 20th second.

$$m = \begin{cases} 2, & 0 \le t < 10 \\ 1.5, & 10 \le t < 20 \\ 1, & 20 \le t \end{cases} \tag{51}$$

The desired trajectory is as following:

$$\begin{cases} x_d = \frac{1}{2}\sin(\frac{\pi t}{4}) \\ y_d = \frac{1}{2}\sin(\frac{\pi t}{8}) \\ z_d = \frac{1}{4} \end{cases} \tag{52}$$

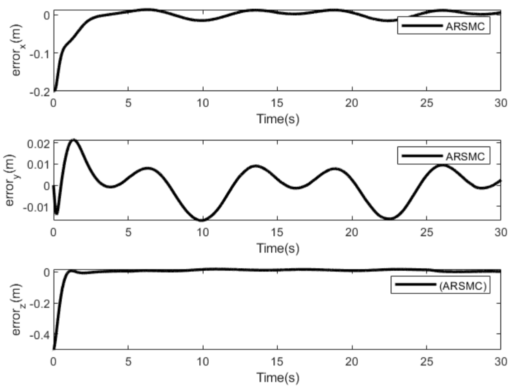

FIGURE 5. **Tracking errors of x, y, z in case 1.**

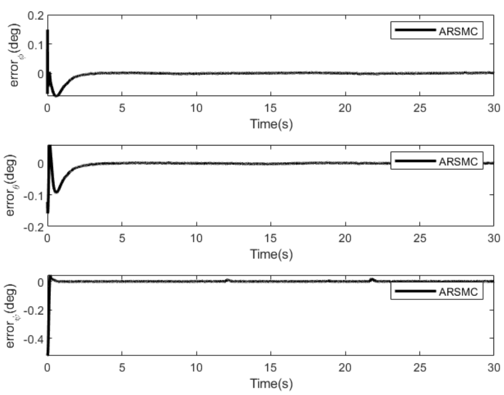

FIGURE 6. **Tracking errors of ϕ, θ, ψ in case 1.**

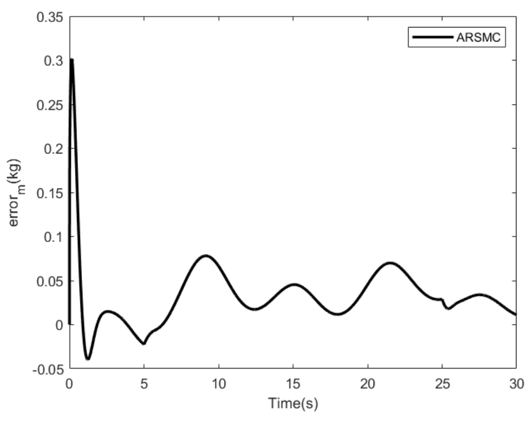

FIGURE 7. **Estimating error of m in case 1.**

After doing the simulations by computer, the flying results are obtained, and shown in the Figs.8-11. Fig.8 is the 3D results of the trajectory tracking. Fig.9 shows the tracking errors of x, y and z. Fig.10 gives the tracking error of ϕ, θ and ψ. The estimation error of m is shown in Fig.11. Fig.8 shows that the controlled QUNV can tracks the desired trajectory successfully. From Figs.9-10, we can obtain, the desired position and angle both can be tracked quickly. However, the maximum position tracking error in z-axis direction reaches 0.14 m, that is mainly for the system receiving a serious disturbance in z-axis direction while a 0.5 kg object is dropped from the QUNV at the 10th and 20th seconds. Fig.11 shows, there is a serious estimating error happening at the dropping time. However, the system can adjust the estimated value of the mass, and reaches a small estimating error, rapidly.

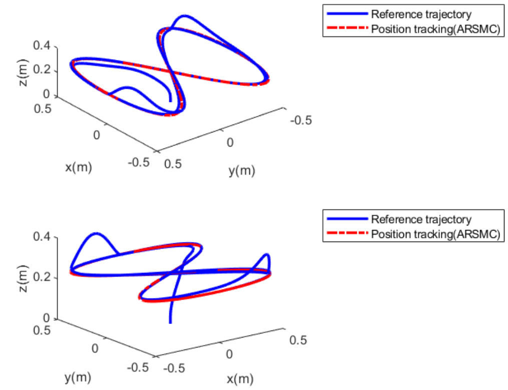

FIGURE 8. **the 3D trajectory tracking results in case 2.**

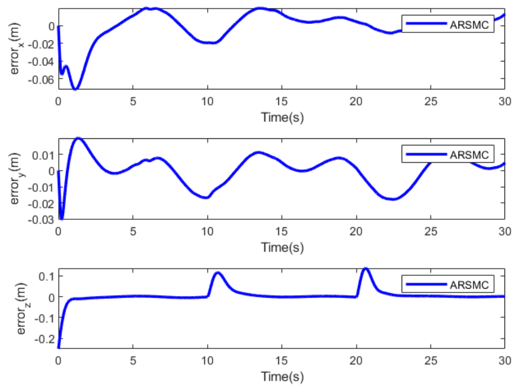

FIGURE 9. **Tracking errors of x, y, z in case 2.**

*Case 3:*Some comparisons of the controller obtained in this paper with some other controllers are given in this case. One compared controller, which combines the ASMC with a SMC, is denoted as controller 1; thereafter, the other compared controller, which combines the ASMC with a BSMC, is denoted as controller 2. The controller obtained in this paper, which combines the ASMC and the ARSMC, is denoted as controller 3. The time-varying mass is defined in (53), in which, the mass is gradually decreased from the 5th second to the 20th second.

$$m = \begin{cases} 2, & 0 \le t < 10 \\ 1.5 - t/40, & 10 \le t < 20 \\ 1, & 20 \le t \end{cases} \tag{53}$$

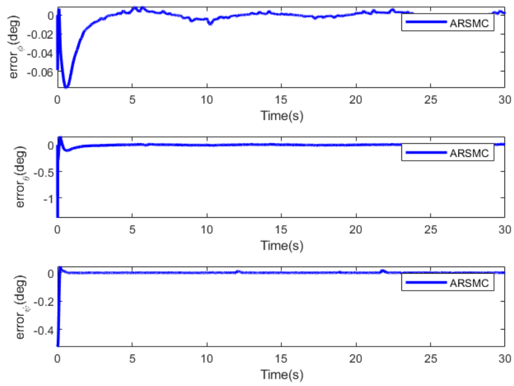

FIGURE 10. Tracking errors of ϕ, θ, ψ in case 2.

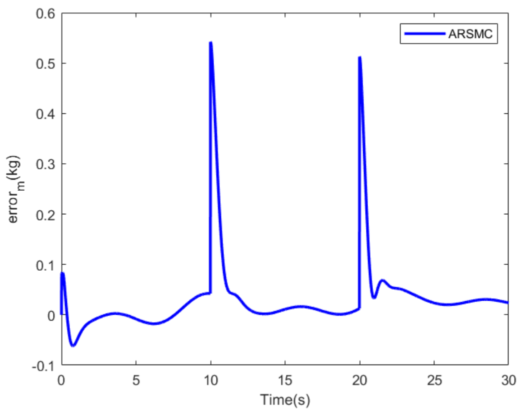

FIGURE 11. Estimating error of the mass m in case 2.

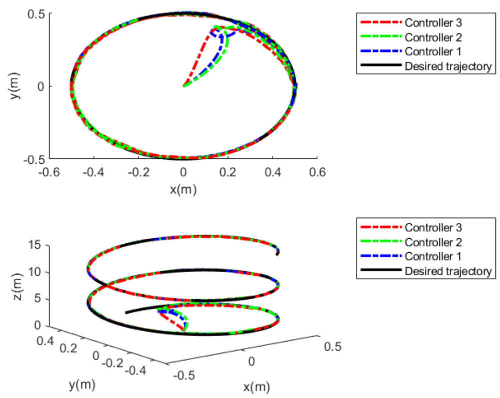

FIGURE 12. The 2D and 3D trajectory tracking results in case 3.

The desired trajectory is as following:

$$\begin{cases} x_d = \frac{1}{2}\sin(\frac{t}{2}) \\ y_d = \frac{1}{2}\cos(\frac{t}{2}) \\ z_d = \frac{1}{2}t \end{cases} \tag{54}$$

After doing the simulations by computer, the obtained results are shown in the Figs.12-14 and Tables 3-4.

Fig.12 and Fig.13 show the three controllers can all control the QAUV, effectively. However, from Fig.14, we can obtain the controller 3 obtained in this paper can achieve

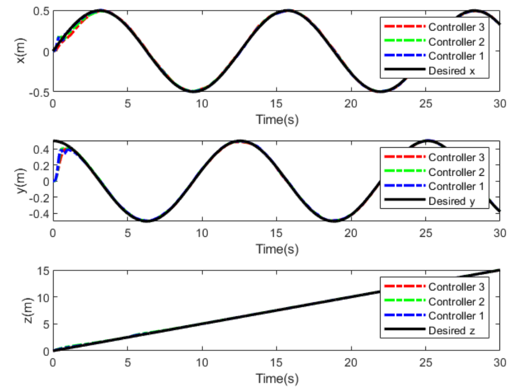

FIGURE 13. Tracking errors of x, y, z in case 3.

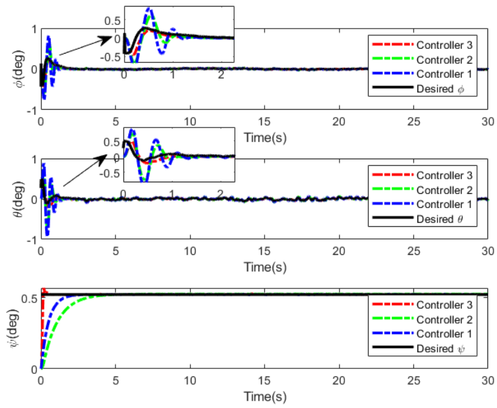

FIGURE 14. Tracking errors of ϕ, θ, ψ in case 3.

TABLE 3. Mean absolute errors of x, y and z in case 3.

Algorithm	$\bar{\tilde{x}}(m)$	$\bar{\tilde{y}}(m)$	$\bar{\tilde{z}}(m)$
Controller 1	0.3247	0.3009	7.512
Controller 2	0.3223	0.3021	7.534
Controller 3	0.3203	0.3000	7.512

$\tilde{x}$, $\tilde{y}$ and $\tilde{z}$ denote the path tracking's mean absolute errors of x, y and z, respectively.

TABLE 4. Responses of the parameters ϕ, θ, and ψ in case 3.

Algorithm	$t_\psi(s)$	θ_{max}	θ_{min}	ϕ_{max}	ϕ_{min}
Controller 1	2.99	0.8825	-0.9382	0.8168	-0.6736
Controller 2	5.25	0.7368	-0.7370	0.6218	-0.6793
Controller 3	0.17	0.4946	-0.2097	0.2060	-0.4597

t_ψ is the rise time of the parameter ψ, h_{max} and h_{min} are the maximum and minimum responses of the parameter h, respectively, where $h = \theta$ and ϕ. The units of h_{max} and h_{min} are radian.

the fastest response speed, compared with the other two controllers. Additionally, due to the inclusion of an ISMC in the controller 3, the angle tracking errors are also less than those obtained by controller 1 and 2. Table 3 shows the mean absolute errors in the x, y, and z channels obtained by the controller 3 are all smaller than those obtained by the other two controllers. thus, the improvements of the tracking performance for the controller 3 is obvious. The system responses in the ϕ, θ and ψ channels are presented in Table 4. Compared with controller 1 and 2, the converge speeds of controller 3 in the three channels are all more fast, obviously.

Additionally, controller 3 can achieves the smaller variations in the θ and ϕ angles. All in all, the controller obtained in this paper can control the time-varying load QUAVs subjected to unknown disturbances, effectively. Moreover, compared with those existing control schemes, such as, SMC and BSMC, etc., the controller with a combination of ASMC and ARSMC can achieves a significant improvement of the flying performance.

V. CONCLUSION

In this paper, an ASMC and ARSMC cascaded controller is presented to solve the trajectory tracking problem for the time-varying load QAUVs subjected to unknown disturbances. The time-varying load and unknown disturbances are estimated by the adaptive laws designed in the ASMC controller, which is used to control the position subsystem. Moreover, the unknown inner-loop disturbances are estimated by a self-turning law designed in the ARSMC controller, which is used to control the attitude subsystem. In order to ensure that the state errors converge to zero, a recursive sliding mode surface is designed, and the desired yaw angle can be tracked, successfully. Moreover, some simulations are performed to demonstrate the robustness and efficiency of the proposed control scheme, and compared with some existing controllers, a better trajectory tracking performance is achieved for the obtained controller in this paper. However, the input delay time and saturation are not considered in this paper, which will be our future works.

REFERENCES

[1] C.-C. Hua, K. Wang, J.-N. Chen, and X. You, "Tracking differentiator and extended state observer-based nonsingular fast terminal sliding mode attitude control for a quadrotor," *Nonlinear Dyn.*, vol. 94, no. 1, pp. 343–354, Oct. 2018.

[2] M. Labbadi, M. Djemai, and S. Boubaker, "A novel non-singular terminal sliding mode control combined with integral sliding surface for perturbed quadrotor," *Proc. Inst. Mech. Eng., I, J. Syst. Control Eng.*, vol. 236, no. 5, pp. 999–1009, May 2022.

[3] B. Wang, Y. Zhang, and W. Zhang, "A composite adaptive fault-tolerant attitude control for a quadrotor UAV with multiple uncertainties," *J. Syst. Sci. Complex.*, vol. 35, no. 1, pp. 81–104, Feb. 2022.

[4] C. Zhu and Y. Song, "Backstepping sliding mode control for quadrotor UAV based on adaptive observer," in *Proc. IEEE 13th Int. Conf. Electron. Inf. Emergency Commun. (ICEIEC)*, Beijing, China, Jul. 2023, pp. 207–212.

[5] J. Wang, Z. Zhao, and Y. Zheng, "NFTSM-based fault tolerant control for quadrotor unmanned aerial vehicle with finite-time convergence," *IFAC-PapersOnLine*, vol. 51, no. 24, pp. 441–446, 2018.

[6] A. Eltayeb, M. F. Rahmat, M. A. M. Basri, and M. S. Mahmoud, "An improved design of integral sliding mode controller for chattering attenuation and trajectory tracking of the quadrotor UAV," *Arabian J. Sci. Eng.*, vol. 45, no. 8, pp. 6949–6961, Aug. 2020.

[7] Z. Chang, H. Chu, and Y. Shao, "Quadrotor trajectory-tracking control with actuator saturation," *Electronics*, vol. 12, no. 3, p. 484, Jan. 2023.

[8] X. Gu, B. Xian, and Y. Wang, "Agile flight for a quadrotor via robust geometry control: Theory and experimental verification," *Int. J. Robust Nonlinear Control*, vol. 32, no. 7, pp. 4236–4250, Jan. 2022.

[9] S. Jamal Haddadi, P. Zarafshan, and M. Dehghani, "A coaxial quadrotor flying robot: Design, analysis and control implementation," *Aerosp. Sci. Technol.*, vol. 120, Jan. 2022, Art. no. 107260.

[10] M. M. Hammad, A. K. Elshenawy, and M. I. El Singaby, "Trajectory following and stabilization control of fully actuated AUV using inverse kinematics and self-tuning fuzzy PID," *PLoS ONE*, vol. 12, no. 7, Jul. 2017, Art. no. e0179611.

[11] S. Zhang, X. Xue, C. Chen, Z. Sun, and T. Sun, "Development of a low-cost quadrotor UAV based on ADRC for agricultural remote sensing," *Int. J. Agricult. Biol. Eng.*, vol. 12, no. 4, pp. 82–87, 2019.

[12] K. Ahmadi, D. Asadi, A. Merheb, S.-Y. Nabavi-Chashmi, and O. Tutsoy, "Active fault-tolerant control of quadrotor UAVs with nonlinear observer-based sliding mode control validated through hardware in the loop experiments," *Control Eng. Pract.*, vol. 137, Aug. 2023, Art. no. 105557.

[13] A. A. Najm and I. K. Ibraheem, "Nonlinear PID controller design for a 6-DOF UAV quadrotor system," *Eng. Sci. Technol., Int. J.*, vol. 22, no. 4, pp. 1087–1097, Aug. 2019.

[14] I. Lopez-Sanchez and J. Moreno-Valenzuela, "PID control of quadrotor UAVs: A survey," *Annu. Rev. Control*, vol. 56, 2023, Art. no. 100900.

[15] G. Tan and Z. Wang, "Stability analysis of recurrent neural networks with time-varying delay based on a flexible negative-determination quadratic function method," *IEEE Trans. Neural Netw. Learn. Syst.*, vol. 10, no. 1, pp. 1–6, Oct. 2023.

[16] H. Thabet, M. Ayadi, and F. Rotella, "Performances comparison between ultra-local model control, integral sliding mode control and PID control for a coupled tanks system," *Int. J. Model., Identificat. Control*, vol. 30, no. 3, p. 219, 2018.

[17] S. Zhong, Y. Huang, and L. Guo, "An ADRCbased PID tuning rule," *Int. J. Robust Nonlinear Control*, vol. 32, no. 18, pp. 9542–9555, Oct. 2022.

[18] C. Wang, L. Quan, S. Zhang, H. Meng, and Y. Lan, "Reduced-order model based active disturbance rejection control of hydraulic servo system with singular value perturbation theory," *ISA Trans.*, vol. 67, pp. 455–465, Mar. 2017.

[19] S. Shao, S. Wang, Y. Zhao, and G. Huang, "Fixed-time robust trajectory tracking control for quadrotor UAV with disturbances," *Trans. Inst. Meas. Control*, vol. 45, no. 7, pp. 1213–1228, Apr. 2023.

[20] J. Liu, W. Gai, J. Zhang, and Y. Li, "Nonlinear adaptive backstepping with ESO for the quadrotor trajectory tracking control in the multiple disturbances," *Int. J. Control, Autom. Syst.*, vol. 17, no. 11, pp. 2754–2768, Nov. 2019.

[21] W.-J. Lin, G. Tan, Q.-G. Wang, and J. Yu, "Fault-tolerant state estimation for Markov jump neural networks with time-varying delays," *IEEE Trans. Circuits Syst. II, Exp. Briefs*, vol. 71, no. 4, pp. 2114–2118, Apr. 2024.

[22] F. Weng, L. Hou, Y. Huang, and H. Wei, "Trajectory tracking control for uncertain agricultural quadrotor based on combining ASMC and NFTSMC," *Int. J. Autom. Control*, vol. 17, no. 1, pp. 635–656, 2023.

[23] Y. Du, P. Huang, Y. Cheng, Y. Fan, and Y. Yuan, "Fault tolerant control of a quadrotor unmanned aerial vehicle based on active disturbance rejection control and two-stage Kalman filter," *IEEE Access*, vol. 11, pp. 67556–67566, 2023.

[24] J. Hu, G. Tan, and L. Liu, "A new result on H_∞ state estimation for delayed neural networks based on an extended reciprocally convex inequality," *IEEE Trans. Circuits Syst. II, Exp. Briefs*, vol. 71, no. 3, pp. 1181–1185, Mar. 2024.

[25] C.-L. Xie, Y.-N Zeng, F.-L. Wang, C. Cai, and X.-C. Zeng, "Design of active disturbance rejection controller for PMSM speed loop based on disturbance compensation," *Small Special Electr. Mach.*, vol. 45, no. 1, pp. 53–56, Jan. 2017.

[26] B. Mu, K. Zhang, and Y. Shi, "Integral sliding mode flight controller design for a quadrotor and the application in a heterogeneous multi-agent system," *IEEE Trans. Ind. Electron.*, vol. 64, no. 12, pp. 9389–9398, Dec. 2017.

[27] X. Shi, Y. Cheng, C. Yin, S. Zhong, X. Huang, K. Chen, and G. Qiu, "Adaptive fractional-order SMC controller design for unmanned quadrotor helicopter under actuator fault and disturbances," *IEEE Access*, vol. 8, pp. 103792–103802, 2020.

[28] F. Weng, Y. Zeng, Z. Yu, Y. Ding, and H. Wang, "Finite-time energy-to-peak control for Markov jump systems with pure time delays," *Meas. Control*, vol. 55, nos. 7–8, pp. 849–860, Aug. 2022.

[29] J.-J. Xiong and G.-B. Zhang, "Global fast dynamic terminal sliding mode control for a quadrotor UAV," *ISA Trans.*, vol. 66, pp. 233–240, Jan. 2017.

[30] X. Fang, L.-M. Wang, and K. Zhang, "High order nonsingular fast terminal sliding mode control of permanent magnet linear motor based on disturbance observer," *Trans. China Electrotechnical Soc.*, vol. 38, no. 2, pp. 409–421, Jan. 2023.

[31] C. Xu and X.-M. Zhao, "Intelligent recursive nonsingular terminal sliding mode control of permanent magnet linear synchronous motor," *Control Theory Appl.*, vol. 39, no. 7, pp. 1242–1250, Jul. 2022.

[32] S. An, S. Yuan, and H. Li, "Adaptive trajectory tracking controller design for a quadrotor UAV with payload variation," *Int. J. Intell. Comput. Cybern.*, vol. 11, no. 4, pp. 496–510, Jul. 2018.
[33] K. S. Brahim, A. E. Hajjaji, N. Terki, and D. L. Alabazares, "Finite time adaptive SMC for UAV trajectory tracking under unknown disturbances and actuators constraints," *IEEE Access*, vol. 11, pp. 66177–66193, 2023.
[34] S. C. Yogi, V. K. Tripathi, and L. Behera, "Adaptive integral sliding mode control using fully connected recurrent neural network for position and attitude control of quadrotor," *IEEE Trans. Neural Netw. Learn. Syst.*, vol. 32, no. 12, pp. 5595–5609, Dec. 2021.
[35] D. J. Almakhles, "Robust backstepping sliding mode control for a quadrotor trajectory tracking application," *IEEE Access*, vol. 8, pp. 5515–5525, 2020.
[36] J. Olguin-Roque, S. Salazar, I. González-Hernandez, and R. Lozano, "A robust fixed-time sliding mode control for quadrotor UAV," *Algorithms*, vol. 16, no. 5, p. 229, Apr. 2023.
[37] Z. Lv, Y. Wu, X.-M. Sun, and Q.-G. Wang, "Fixed-time control for a quadrotor with a cable-suspended load," *IEEE Trans. Intell. Transp. Syst.*, vol. 23, no. 11, pp. 21932–21943, Nov. 2022.
[38] M. Ryll, H. H. Bulthoff, and P. R. Giordano, "A novel overactuated quadrotor unmanned aerial vehicle: Modeling, control, and experimental validation," *IEEE Trans. Control Syst. Technol.*, vol. 23, no. 2, pp. 540–556, Mar. 2015.
[39] S. Wang, J. Chen, and X. He, "An adaptive composite disturbance rejection for attitude control of the agricultural quadrotor UAV," *ISA Trans.*, vol. 129, pp. 564–579, Oct. 2022.
[40] W. Yang, G. Cui, J. Yu, C. Tao, and Z. Li, "Finite-time adaptive fuzzy quantized control for a quadrotor UAV," *IEEE Access*, vol. 8, pp. 179363–179372, 2020.
[41] H. Maqsood and Y. Qu, "Nonlinear disturbance observer based sliding mode control of quadrotor helicopter," *J. Electr. Eng. Technol.*, vol. 15, no. 3, pp. 1453–1461, Apr. 2020.
[42] J.-J. Xiong and E.-H. Zheng, "Position and attitude tracking control for a quadrotor UAV," *ISA Trans.*, vol. 53, no. 3, pp. 725–731, May 2014.
[43] X. Zou, Z. Liu, H. Gao, and W. Zhao, "Trajectory tracking control of quadrotor under variable payloads with model-free controller and sliding mode control technology," *Aircr. Eng. Aerosp. Technol.*, vol. 93, no. 10, pp. 1533–1546, Nov. 2021.
[44] F. Wang, Z. Ma, H. Gao, C. Zhou, and C. Hua, "Disturbance observer-based nonsingular fast terminal sliding mode fault tolerant control of a quadrotor UAV with external disturbances and actuator faults," *Int. J. Control, Autom. Syst.*, vol. 20, no. 4, pp. 1122–1130, Apr. 2022.
[45] Y. Zhong, Y. Zhang, W. Zhang, J. Zuo, and H. Zhan, "Robust actuator fault detection and diagnosis for a quadrotor UAV with external disturbances," *IEEE Access*, vol. 6, pp. 48169–48180, 2018.
[46] O. Mechali, L. Xu, Y. Huang, M. Shi, and X. Xie, "Observer-based fixed-time continuous nonsingular terminal sliding mode control of quadrotor aircraft under uncertainties and disturbances for robust trajectory tracking: Theory and experiment," *Control Eng. Pract.*, vol. 111, Jun. 2021, Art. no. 104806.
[47] L.-J. Wang, W.-C. Deng, J.-K. Liu, and R. Mei, "Adaptive sliding mode trajectory tracking control of quadrotor UAV with unknown control direction," in *Proc. 11th Int. Conf. Modeling, Identificat. Control (ICMIC)*, Singapore. Cham, Switzerland: Springer, Dec. 2019, pp. 597–607.
[48] M. Boukattaya, N. Mezghani, and T. Damak, "Adaptive nonsingular fast terminal sliding-mode control for the tracking problem of uncertain dynamical systems," *ISA Trans.*, vol. 77, pp. 1–19, Jun. 2018.
[49] Z.-Q. Liu, W.-Y. Cai, M.-Y. Zhang, and S.-S Lv, "Adaptive nonsingular fast terminal sliding-mode control for the tracking problem of uncertain dynamical systems," *J. Mar. Sci. Eng.*, vol. 10, no. 6, p. 795, Jun. 2022.
[50] R. Xiong, L. Li, C. Zhang, K. Ma, X. Yi, and H. Zeng, "Path tracking of a four-wheel independently driven skid steer robotic vehicle through a cascaded NTSM-PID control method," *IEEE Trans. Instrum. Meas.*, vol. 71, pp. 1–11, 2022.
[51] Z. Sun, J. Zheng, H. Wang, and Z. Man, "Adaptive fast non-singular terminal sliding mode control for a vehicle steer-by-wire system," *IET Control Theory Appl.*, vol. 11, no. 8, pp. 1245–1254, May 2017.
[52] L. Chen, Z. Liu, H. Gao, and G. Wang, "Robust adaptive recursive sliding mode attitude control for a quadrotor with unknown disturbances," *ISA Trans.*, vol. 122, pp. 114–125, Mar. 2022.
[53] L. Yang and J. Yang, "Nonsingular fast terminal sliding-mode control for nonlinear dynamical systems," *Int. J. Robust Nonlinear Control*, vol. 21, no. 16, pp. 1865–1879, Nov. 2011.

FALU WENG received the Ph.D. degree from Zhejiang University, China, in 2012. He is currently an Associate Professor with the School of Electrical Engineering and Automation, Jiangxi University of Science and Technology, Ganzhou, China. His research interests include adaptive control, robust control, and system modeling and simulation.

HUI WEI received the B.E. degree in automation from Jiangxi University of Science and Technology, Ganzhou, China, in 2021. He is currently pursuing the M.S. degree with the School of Electrical Engineering and Automation, Jiangxi University of Science and Technology, Ganzhou. His main research interest includes sliding mode control of quadrotor UAVs.

JIANYI HU received the B.E. degree from the University of Science and Technology, Liaoning, Anshan, China, in 2009. He is currently a Teacher with the School of Jiangxi New Energy Technology Institute, Xinyu, China. His main research interests include automation and embedded systems.

LU ZENG received the M.S. degree from Jiangxi University of Science and Technology, Ganzhou, Jiangxi, China, in 2005. She is currently an Associate Professor with the School of Electrical Engineering and Automation, Jiangxi University of Science and Technology, Ganzhou. Her research interests include embedded systems, robust control, and system modeling and simulation.

RUCHUN WEN received the M.S. degree from Jiangxi University of Science and Technology, Ganzhou, Jiangxi, China, in 2008. She is currently an Associate Professor with the School of Electrical Engineering and Automation, Jiangxi University of Science and Technology, Ganzhou. Her research interests include adaptive control, data analysis, and system modeling.